Proc. Natl. Acad. Sci. USA
Vol. 91, pp. 7698–7702, August 1994
Neurobiology

Lasting potentiation of inhibition is associated with an increased number of γ-aminobutyric acid type A receptors activated during miniature inhibitory postsynaptic currents

(hippocampus/granule cell/dentate gyrus/kindling/epilepsy)

THOMAS S. OTIS*, YVES DE KONINCK, AND ISTVAN MODY†

Department of Anesthesiology and Pain Management, University of Texas Southwestern Medical Center, Dallas, TX 75235-9068

Communicated by A. J. Hudspeth, April 18, 1994

ABSTRACT **Whole-cell patch-clamp recordings unveiled a substantial increase in the amplitude, but no change in the frequency, of miniature inhibitory postsynaptic currents (mIPSCs) in dentate gyrus granule cells following chronic epilepsy induced by kindling. This novel and persistent enhancement of γ-aminobutyric acid type A ($GABA_A$) receptor-mediated inhibition lasted for at least 48 hr following its induction. Nearly a doubling of the number of activated functional postsynaptic $GABA_A$ receptor channels during mIPSCs without any change in single-channel conductance or kinetics could be demonstrated using nonstationary fluctuation analysis. As postsynaptic $GABA_A$ receptors are likely to be pharmacologically saturated by the transmitter concentration in the cleft, incrementing the number of functional receptor channels may be the most effective means to augment inhibition in the mammalian brain.**

A fundamental mechanism for plasticity in the central nervous system (CNS) is the alteration in the gain of synaptic transmission. Activity-dependent plastic changes are mainly confined to excitatory synapses and may be required for learning and memory (1) or, under more severe circumstances, may lead to pathological states of excitability (2, 3). In contrast, inhibitory synapses of the mammalian CNS are known to exhibit only short-term plasticity, which, with a few exceptions in cerebellar Purkinje cells, usually results in a diminished inhibition. For example, in Purkinje cells, Ca^{2+} entry induced by repetitive depolarizing pulses can cause a short-term (<10 min) increase in the sensitivity to exogenously applied γ-aminobutyric acid (GABA) and a transient (<1 min) retrograde inhibition of synaptic terminals releasing GABA (4). Moreover, repetitive stimulation of climbing fibers leads, presumably through Ca^{2+} accumulation, to a rebound potentiation of spontaneous inhibitory postsynaptic currents (IPSCs) lasting over an hour (5). A similar time course of potentiation of the glycinergic inhibitory synapse has been observed in teleost Mauthner cells (6). So far, no such potentiation of spontaneous GABAergic synaptic events has been observed in the cerebral cortex. In fact, the opposite, an activity-dependent reduction of inhibition, appears to be the rule. In the hippocampal CA1 region, repetitive firing of pyramidal cells produces a transient Ca^{2+}-dependent decrease of the amplitude of spontaneous IPSCs (7) and tetanic stimulation of the stratum radiatum *in vitro* also reduces GABAergic IPSPs (8). Similarly, in the CA3 region, the efficacy of recurrent inhibition is diminished following afferent fiber stimulation (9). Finally, during tetanic stimulation, activation of $GABA_B$ autoreceptors causes a transient decrease of GABA release leading to long-term potentiation (10, 11).

Lasting activity-dependent decrease in inhibition has been also associated with epileptiform activity (12, 13). Yet, following chronic epilepsy induced by kindling, there is a paradoxical increase in paired-pulse depression of excitatory responses in the dentate gyrus, which may last for weeks (14–16). In addition, increases in GABA, muscimol, or benzodiazepine binding have also been reported in the kindled dentate gyrus (17–20). Generally, an increase in inhibition may occur through enhanced transmitter release, a more synchronized release, some modification of postsynaptic channel properties, or an increase in the number of postsynaptic channels. A recent model of GABAergic synaptic transmission in dentate gyrus granule cells (21) favors the hypothesis that at these synapses, the ratio of transmitter-to-receptor concentration is high in contrast to what has been observed at the neuromuscular junction (22, 23). This model thus predicts an increase in receptor number on the postsynaptic membrane to be most effective in leading to an increased amplitude of synaptic currents.

By using high-resolution recordings and the newly developed nonstationary fluctuation analysis of synaptic currents (24–27), we demonstrate that an increase in functional receptor number in kindled granule cells underlies an augmented $GABA_A$ receptor-mediated inhibition that may last in excess of 48 hr.

MATERIALS AND METHODS

Kindling. The procedure for the daily kindling of male Wistar rats through the hippocampal commissures has been presented elsewhere (2, 3). The 11 control cells were taken from three age-matched and two sham-implanted animals. The 11 kindled cells were obtained from four fully kindled animals, each with 5–12 stage 5 motor seizures (28), sacrificed 24–48 hr after the last seizure. Such animals have no spontaneous seizures, and there is no evidence of epileptic activity in the kindled slices under physiological conditions (also see ref. 29).

Slices and Solutions. Coronal half-brain slices (400 μm thick) were prepared from control and kindled rats (350–400 g) as described (30, 31). The artificial cerebrospinal fluid used to perfuse the slices at 32°C contained (in mM) 126 NaCl, 5 KCl, 2 $CaCl_2$, 2 $MgCl_2$, 26 $NaHCO_3$, 1.25 NaH_2PO_4, 10 D-glucose, 0.01 6-cyano-7-nitroquinoxaline-2,3-dione (CNQX; Tocris Neuramin, Bristol, U.K.), 0.04 D-2-amino-5-phosphonovaleric acid (D-AP5; Cambridge Research Biochemicals or Tocris Neuramin), and 0.001 tetrodotoxin (TTX; Calbiochem) and

The publication costs of this article were defrayed in part by page charge payment. This article must therefore be hereby marked "*advertisement*" in accordance with 18 U.S.C. §1734 solely to indicate this fact.

Abbreviations: IPSC, inhibitory postsynaptic current; mIPSC, miniature IPSC; GABA, γ-aminobutyric acid; CNQX, 6-cyano-7-nitroquinoxaline-2,3-dione; D-AP5, D-2-amino-5-phosphonovaleric acid; TTX, tetrodotoxin; CNS, central nervous system.

*Present address: Department of Neurophysiology, University of Wisconsin, Madison, WI 53706.
†To whom reprint requests should be addressed.

was continuously bubbled with 95% O_2/5% CO_2 (pH 7.35 ± 0.05). Intracellular solutions contained (in mM) 140 CsCl, 10 Hepes, and 2 $MgCl_2$ (pH adjusted to 7.2 with CsOH; 265–285 mosM). Calcium chelators were not used as they do not improve recordings of miniature IPSCs (mIPSCs) (30); instead, they may mask changes in the endogenous Ca^{2+} handling capacity of granule cells (32).

Recording and Data Acquisition. Tight-seal, whole-cell voltage-clamp recordings were made from granule cells of the dentate gyrus. Access resistance through the patch electrode was compensated 60–80% using an Axopatch 200A patch-clamp amplifier (Axon Instruments, Foster City, CA) and was monitored throughout each experiment. The average access resistances were not different between recordings in control and kindled cells (11.7 ± 1.2 MΩ vs. 10.3 ± 0.7 MΩ, respectively). Recordings were low-pass filtered 2–5 kHz (−3 decibels, eight-pole Bessel, Frequency Devices 9002) and sampled at 4–50 kHz on computer (CDR software; courtesy of J. Dempster, University of Strathclyde, Glasgow, U.K.). Detection of individual mIPSCs was done off-line using a previously described software trigger (30). Experimental values are reported as mean ± SEM unless otherwise noted.

Nonstationary Noise Analysis. For the nonstationary noise analysis, events were low-pass filtered at 4 kHz and sampled at 30 kHz. The following criteria were used for selection. (*i*) A higher detection threshold was set to facilitate analysis by focusing on large events. (*ii*) Only events with rapid 10–90% rise times (100–600 μs) were selected to ensure that the mIPSCs were from a population of synapses with similar kinetics and to minimize the space clamp error and electronic filtering. (*iii*) Traces containing multiple events were discarded. Of all events detected in control and kindled neurons, 21.2% ± 2.0% and 22.3% ± 1.9%, respectively, satisfied the above criteria and were consequently used for the nonstationary analysis. Because of the higher detection threshold, these events had larger average conductances than the population mean shown in Fig. 1*C*, but the ratio of conductances between kindled and control mIPSCs was the same.

The selected events were aligned by their fastest rate of rise, averaged, and the ensemble average current (I_m) was scaled to the peak of individual mIPSC before being subtracted from the raw traces (26, 27). Segments of fixed length (20 ms) starting at the peak of mIPSCs were then divided into 20 bins of equal size on the amplitudes scale. Within each of the 20 bins, the variance (σ^2) of the current around I_m was computed and baseline σ^2 was subtracted. Baseline σ^2 was obtained from the current before the start of each mIPSC. The values of σ^2 were plotted against I_m, binned, and the relationship $\sigma^2 = iI_m - I_m^2/N$ was fit (least-squares method) to the data points to obtain i, the unitary current, and N, the number of channels responsible for generating the mIPSC (27).

The use of the scaling method mentioned above provided accurate estimates of the unit conductance (γ) (26, 27) by avoiding the bias introduced by the least-squares scaling method (25), which, by definition, underestimates the large variance during the decay phase of mIPSCs (see appendix in ref. 25). Such scaling method is, however, based on the assumption that most channels activated during a synaptic current open synchronously at its peak. Several factors may cause deviation from this ideal condition, precluding accurate estimation of N (26, 27, 33). In a recent study (27), we have determined that, in the case of granule cell $GABA_A$ mIPSCs, the assumption that most channels are open at the peak of the current is correct, and thus accurate estimates of N can be obtained. Another assumption of noise analysis is that the channels have only one open conductance level. Because several subconductance levels may be involved, the calculated γ refers to a weighted unit conductance. However, cell-attached recordings of single $GABA_A$ channel activity in adult dentate gyrus granule cells demonstrated no significant subconductance levels (Y.D.K. and I.M., unpublished results).

Simulation of mIPSCs. Computer simulations of mIPSCs were used as described in detail by De Koninck and Mody (27). Briefly, stochastic simulations of individual mIPSCs were obtained through one of the following three- or four-state kinetic models: $C \rightleftharpoons C \rightleftharpoons O$, $C \rightleftharpoons O \rightleftharpoons C$, and $C \rightleftharpoons C \rightleftharpoons C \rightleftharpoons O$. Transition probabilities were derived from their corresponding matrices of transition rates (27, 34). Transmitter concentration was modeled as instantaneously rising and exponentially decaying ($0 < \tau < 0.5$ ms). The mIPSCs (100–3000) were constructed by the addition of 10–500 traces of simulated channel activity. The number of channels per mIPSC was determined by using standard Gaussian, binomial, or Poisson deviates (35). Pseudo-random noise was added to the traces using a standard Gaussian deviate (35) and traces were then fed through a digital Gaussian filter (36). A wide range of rate constants was used to generate IPSCs with varying rise and decay time constants. These computer simulations have shown that, for currents with kinetics similar to those of granule cell mIPSC, the method provides accurate estimation of N and γ (27).

RESULTS

Tight-seal, whole-cell recordings were obtained from dentate gyrus granule cells in conventional adult rat brain slices (30, 31) prepared either from control animals or from rats that had received daily electrical stimulation (kindling) of the hippocampal commissures (2, 3, 28). All recordings were done in the presence of CNQX, D-AP5, and TTX. The mIPSCs reversed at the Cl^- equilibrium potential (0 mV using CsCl-filled electrodes) and were blocked by the competitive $GABA_A$ receptor antagonists (30) bicuculline (10 μM) and SR-95531 (1 μM). The frequency, mean amplitude, and kinetics of mIPSCs were constant over the course of the recordings (30).

To ensure that the estimates of mean amplitude and frequency were not biased by failure to detect small events, we analyzed >500 events recorded in each cell at two different holding potentials (−50 mV and −70 mV; Fig. 1 *A* and *B*). Cells were only included in the analysis if no significant differences could be detected in mIPSC frequency or conductance (Fig. 1*B*) at the two holding potentials. The frequencies of mIPSCs in control and kindled preparations were comparable (14.2 ± 2.8 Hz in control and 12.8 ± 1.8 Hz in kindled; $n = 7$ in each group). The mean conductance at the peak of mIPSCs was significantly ($P < 0.01$) larger in kindled granule cells (175% of control; Fig. 1*C*). Such increases in mIPSC amplitude (or conductance) may result from a variety of pre- or postsynaptic factors.

If the increase in mIPSC size results from a presynaptic mechanism, there are essentially two possibilities: (*i*) an increase in vesicular transmitter content or (*ii*) an enhanced synchronization of presynaptic release. The first mechanism is unlikely in view of several detailed and realistic modeling studies of GABAergic transmission (21, 37) demonstrating that large changes in transmitter release would result only in small increases in mIPSC size (also see ref. 33). Nevertheless, such presynaptic mechanism or a change in the type of vesicle being released may have some contribution to the enhanced mIPSC conductance. The second possibility—synchronous release—may take place at the same or at a different bouton. At a given bouton, vesicular synchronization of release would have analogous effects to the increased vesicular content discussed above. The possibility of a coincident release in two or more boutons, whereby large mIPSCs would arise from summation of two or more elementary synaptic currents, was examined by analyzing the

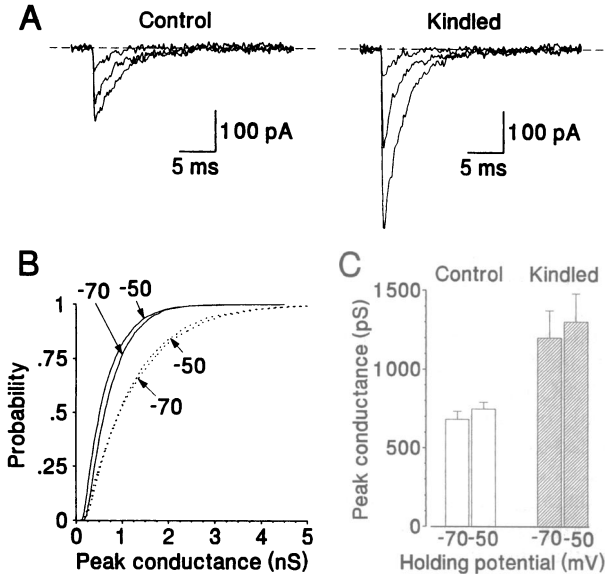

FIG. 1. Enhancement of $GABA_A$ receptor-mediated mIPSC amplitude following kindling. (*A*) Representative raw traces of mIPSCs recorded at comparable holding potentials (−70 mV) in granule cells from an electrode-implanted control and a kindled animal, respectively (records were low-pass filtered at 2 kHz and sampled at 20 kHz). (*B*) The cumulative probability plots of mIPSC conductances were obtained as follows. Five hundred successive mIPSCs each were randomly selected at two holding potentials (−50 and −70 mV). This procedure was repeated in recordings from 7 control and 7 kindled neurons and the resulting 3500 conductance measurements for each case were plotted as cumulative probability distributions (solid lines for control neurons and dotted lines for kindled neurons). The increase in mIPSC conductance following kindling equally affects both small and large amplitude events. To ensure that the mean amplitude estimate was not biased by our inability to detect small events because of impaired resolution, we routinely compared mIPSC frequency at two different holding potentials. In 14 of 22 neurons, the frequency of events detected at −50 mV differed by <15% from that recorded at −70 mV. Thus, in these 14 neurons, the signal-to-noise ratio of the recording was considered sufficient to detect the smallest of events at −50 mV and consequently to accurately calculate mIPSC conductance. In the remaining 8 neurons, the frequency of mIPSCs detected at −70 mV was slightly higher than that measured at −50 mV, suggesting that smaller mIPSCs were buried in the noise at −50 mV. (*C*) The average conductance measured at the peak of mIPSCs was significantly ($P < 0.01$; two-tailed *t* test) larger in kindled granule cells regardless of the holding potential. When the remaining 8 neurons were included in the analysis, the average conductances were 1086 ± 134 pS (at −70 mV), 1152 ± 146 pS (at −50 mV) and 746 ± 78 (at −70 mV), 838 ± 79 (at −50 mV) for kindled and control neurons, respectively ($n = 11$ for both groups). Although the apparent conductance was larger at −50 mV because of the bias toward larger events, the control and kindled data are still significantly different from each other ($P < 0.01$; two-tailed *t* test). The reversal potential of mIPSCs was unaltered following kindling.

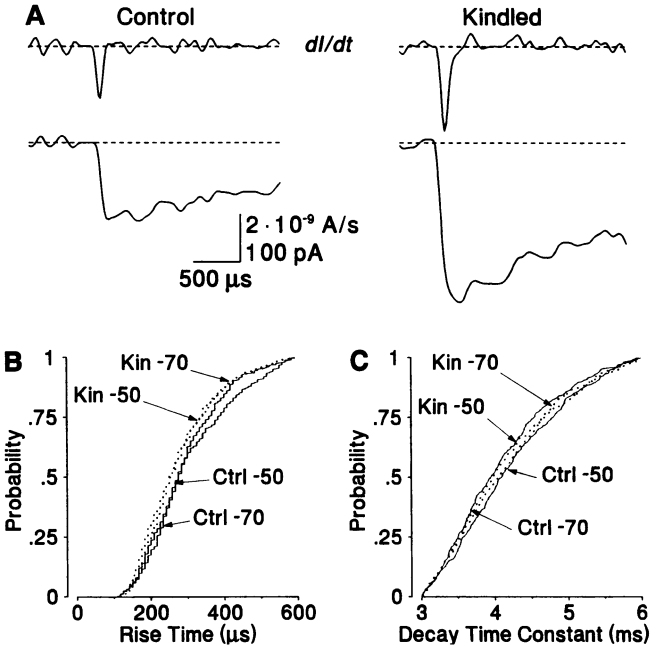

FIG. 2. Rise times and decay time constants of mIPSCs are not altered by kindling. (*A*) Two examples of the rising phases and the derivatives (*dI/dt*) of large mIPSCs selected for nonstationary fluctuation analysis (see text for details) in a control and a kindled neuron, respectively. Note the expanded time scale (low-pass filtered at 5 kHz and sampled at 50 kHz). The large-amplitude mIPSC in the kindled neuron (>300 pA) has no inflection point on the rising phase of the synaptic current and has no "notch" on the differentiated trace to suggest a synchrony of two separate events. (*B* and *C*) Cumulative probability plots of the rise times (*B*) and the decay time constants (*C*) of 7 × 65 mIPSCs satisfying the selection criteria for nonstationary noise analysis (see text for details). The events used for the nonstationary fluctuation analysis at two holding potentials were chosen at random from each of the seven control (Ctrl; solid lines) and seven kindled (Kin; dotted lines) cells (i.e., each of the four curves represents 455 measurements). There are no significant changes in the rise times and decay time constants following kindling.

rise time and decay kinetics of mIPSCs. Unless such release is highly synchronous, the summation of several mIPSCs should produce a lengthening of the rise time and possibly a prolongation of the decay time constant. Kindling, however, did not change the rise time (Fig. 2 *A* and *B*) or decay kinetics (Fig. 2*C*) of mIPSCs. Mean mIPSC rise times (10–90%) recorded at −70 mV in control and kindled cells were 507 ± 58 µs and 449 ± 44 µs, respectively. Decay time constants at the same membrane potential were 4.19 ± 0.24 ms and 4.19 ± 0.43 ms in control and kindled neurons, respectively. The rise time and peak amplitude of mIPSCs were not correlated to each other (not shown), and large events had no inflection points or "notches" during their rising phases as it would be expected from small jitters during synchrony (Fig. 2*A*). This finding is consistent with the hypothesis that large mIPSCs are not composed of multiple synchronized elementary events. The synchronization of release across terminals would have to be more rapid than the resolution of our recording system (74 µs). Furthermore, the similarity between the frequency of events in control and kindled preparations would not be expected if an increased synchronization were responsible for the increased mIPSC conductance.

On the postsynaptic side, the increase in mIPSC amplitude may result from a change in the average number of postsynaptic channels (N), their unitary conductance (γ), the probability of being open at the peak of the response (P_o), or any combination thereof. To examine these possibilities, we have adapted the nonstationary fluctuation analysis developed by Sigworth (24). We have modified the approach used by Robinson *et al.* (25) to more accurately resolve the number of functional $GABA_A$ receptor channels underlying mIPSCs (Fig. 3*A*). Extensive analyses of computer-simulated mIPSCs convincingly demonstrated the precision of the nonstationary analysis (e.g., Fig. 3*B*; see ref. 27 for details).

The congruence of the nonstationary fluctuation analysis technique for estimating γ and N in control and kindled neurons (Fig. 3 *C* and *D*) was verified by implementing the analysis at two different membrane potentials. Within each experimental group (control or kindled), neither γ nor N changed with membrane potential (Fig. 3 *E* and *F*). This is to be expected, as single-channel conductance is linear in the −50 to −70 mV range (38). The average values for γ obtained

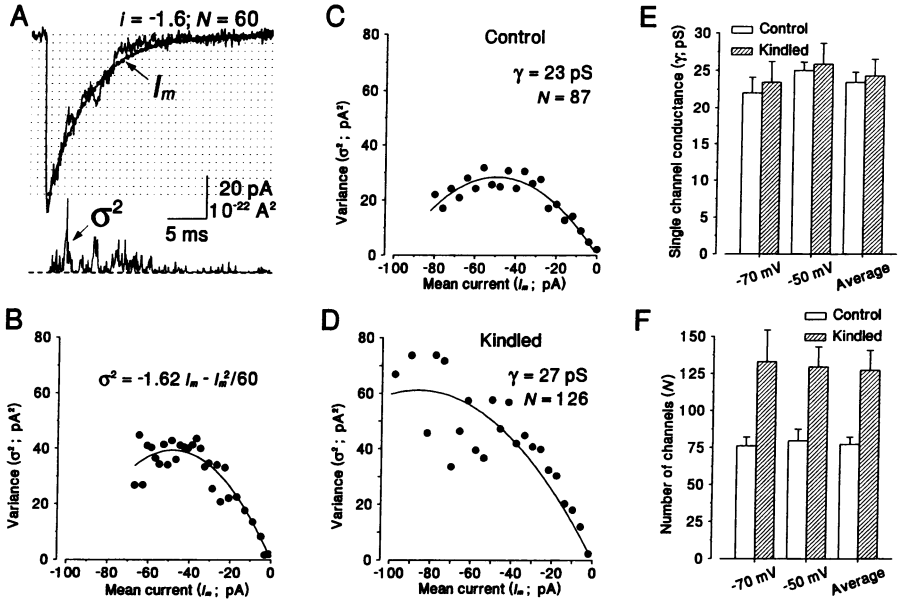

FIG. 3. Enhancement of the mIPSC amplitude is associated with an increase in the number (N) but no change in the unitary conductance (γ) of postsynaptic $GABA_A$ receptor channels. Analyses of hundreds of simulated mIPSCs ensured that the relationship between mean current amplitude vs. current variance provided accurate information about N and γ. (*A*) Nonstationary fluctuation analysis was performed on 150–200 simulated or real mIPSCs (see text for details). The variance resulting from subtraction of the scaled I_m from an individual mIPSC simulated with $i = -1.6$ pA and $N = 60$ is shown to illustrate σ^2 as a function of time. (*B*) A parabola of the form $\sigma^2 = iI_m - I_m^2/N$ (where I_m is the mean current, i is the unitary current, and N is the number of channels) was fitted by least-squares simplex method to the points of the I_m vs. σ^2 plot obtained from 150 simulated mIPSCs like that shown in *A*. Accurate estimates of i (−1.62 pA vs. −1.6 pA used for simulation) and N (60 vs. 60 used for simulation) were obtained for this and all other simulations that involved mIPSCs with realistic channel kinetics (see text for details). (*C* and *D*) Examples of I_m vs. σ^2 plots from mIPSCs recorded in a control (*C*) and a kindled (*D*) neuron. (*E*) To ensure that the technique gave consistent estimates of γ, we compared estimates obtained at two different holding potentials. The values obtained for γ were constant at both −50 and −70 mV. In two cells, additional measurements at −85 mV and +40 mV gave values similar to those obtained at −50 and −70 mV (not shown). (*F*) In contrast to γ, the average number of channels (N) underlying mIPSCs in kindled granule cells was 1.65-fold greater than that in control neurons. As expected, the value of N did not vary with the holding potential.

for control (23.4 ± 1.4 pS) and kindled (24.3 ± 2.2 pS) $GABA_A$ receptor channels are in good agreement with previous reports of the predominant γ in these neurons (refs. 37 and 38; also see discussion in ref. 27). As there was no significant difference in γ between control and kindled $GABA_A$ receptor channels, the change in mIPSC conductance should reflect an increase in N underlying mIPSCs. Indeed, N was significantly increased (165% of control) in the kindled group (Fig. 3*F*). Thus, an increased number of functional $GABA_A$ receptor channels appears to account fully for the enhanced amplitude of mIPSCs in kindled granule cells.

DISCUSSION

At central GABAergic synapses it is N rather than the vesicular transmitter content that is likely to limit the size of elementary synaptic currents. The alternative hypothesis that the vesicular concentration of transmitter is the limiting factor is highly unlikely. This idea is based on elaborate modeling studies of central postsynaptic currents (21, 33, 37) and takes into account the low number of channels underlying each IPSC, the necessary high concentration of GABA in the synaptic cleft to produce the fast rise time of synaptic currents (39), the overwhelming number of GABA molecules contained in a single synaptic vesicle with respect to the number of channels activated, the low quantal variance of evoked IPSCs, and the skewed amplitude distribution of mIPSCs (21, 30, 37). Therefore, in contrast to the neuromuscular junction (22, 23), transmission at mammalian CNS synapses involves activating nearly all of the tens of postsynaptic receptor channels that are pharmacologically saturated by the transmitter concentration in the cleft (21, 33). Based on the current understanding of the $GABA_A$ synapse, it appears that alterations in transmitter concentration or open probability of the channels have little effect on the size of the mIPSCs (27). It has been proposed that receptors aggregate in a characteristic manner forming quantal groups of a constant number and that their number determines the size of mIPSCs (40). In such circumstances, the simplest way of enhancing the efficacy of released GABA may be to increase the number of functional $GABA_A$ receptor channels. Alternatively, as the conductance of $GABA_A$ channels depends on subunit assembly (41), another way to enhance the amplitude of mIPSCs would be to change the molecular composition of the receptors. Consistent with previous binding studies following kindling (17–19) and with the accepted model, an increase in the number of postsynaptic $GABA_A$ receptors would appear to be the mechanism whereby plasticity is expressed at the inhibitory synapses on granule cells.

The skewed (and perhaps multiquantal) amplitude distribution of mIPSCs may reflect the presence of a variable number of quantal aggregates on the postsynaptic membrane opposite a bouton, and the release of a single vesicle may activate one or several of these aggregates (40). However, at glycinergic synapses of goldfish Mauthner cells, the apparent multiquantal distribution of TTX-insensitive IPSPs may result from the synchronous release of two or more vesicles at adjacent active zones within single boutons (42). This hypothesis was based on the single Gaussian (nonskewed) distribution of IPSP amplitudes after lowering the probability of release by reducing extracellular calcium. Thus, the larger amplitude of mIPSCs following kindling may be secondary to an enhanced synchronous release of vesicles at adjacent active zones. Several observations are inconsistent with this scenario being responsible for the enhancement seen following kindling. (*i*) In granule cells of the dentate gyrus, mIPSCs still appear to have a skewed amplitude distribution after

lowering the extracellular calcium concentration (30). (*ii*) The absence of inflection points on the rising phase of mIPSCs (Fig. 2*A*) tends to rule out the possibility of larger events resulting from the release of multiple vesicles. If such release were to exist, it would have to be highly synchronous, and currently there is no known mechanism to account for such rapid synchrony of release in the absence of action potentials. (*iii*) No change in the frequency of events was observed after kindling, contrary to what would be expected to result from an increased synchronization. (*iv*) Examination of the amplitude distributions of mIPSCs indicates a general shift of the distribution toward higher amplitudes after kindling, with no apparent alteration in the nature of the distribution (Fig. 1*B*). If a specific increase in synchrony took place, a change in the relative distribution of amplitudes would also be expected. Namely, a decrease in the relative number of small events vs. an increase in the relative number of large events should occur, as has been reported in a model of mEPSC potentiation (43). In summary, it appears unlikely that an action potential independent synchrony of vesicular release can account for the potentiation of mIPSCs following kindling.

The increase in amplitude of GABAergic mIPSCs persists for at least 48 hr after the final kindling stimulation and may explain the paradoxical enhancement of paired-pulse depression in the kindled dentate gyrus (14–16) that lasts for weeks following cessation of stimulation. However, the exact mechanism for such recruitment or uncovering of dormant postsynaptic $GABA_A$ receptor channels during kindling remains unknown. There are 60–80 functional $GABA_A$ receptor channels open at the peak of a given large mIPSC. These channels represent >80% of the total number of activated receptor channels pharmacologically saturated by the transmitter concentration in the cleft (33). This is based on simulation studies consistently showing the lowest variance resulting from stochastic channel behavior at the peak of mIPSCs (27, 33). Thus, under control conditions there are few, if any, spare functional postsynaptic receptors to be recruited into activation during a mIPSC following kindling. Yet, if the diameter of a $GABA_A$ receptor channel is around 8.5 nm, like that of acetylcholine receptors (44, 45), then the postsynaptic region of GABA synapses on granule cells (46) is sufficiently large to accommodate many more than 60–80 receptor channels. It follows that partially assembled or nonfunctional (perhaps desensitized) receptor channels may already be present in the postsynaptic membrane. Alternatively, kindling may have induced the *de novo* synthesis or the assembly of functional receptor channels (e.g., phosphorylation of unassembled γ subunits of the acetylcholine receptor increases the efficiency of subunit assembly; ref. 47) in the postsynaptic membrane. It is also plausible that whole clusters of receptor channels may be inserted as a "bunch" into the postsynaptic membrane. The gephyrin-dependent clustering of glycine receptors in cultured spinal cord neurons (48) is consistent with this possibility.

It will be a challenge to elucidate just how the number of postsynaptic $GABA_A$ receptor channels activated during mIPSCs increases after kindling. Such increase may be the most prevalent means for augmenting the strength of inhibitory neurotransmission in the mammalian CNS. It remains to be determined whether similar mechanisms play a role in the long-term potentiation of glutamatergic synapses where an increase in miniature excitatory postsynaptic currents has also been reported (49).

We thank Dr. J. Dempster for providing the Strathclyde Electrophysiology Software and Dr. I. Soltesz, J. T. Palmer, and J. Datte for help with the surgery and kindling. This work was supported by National Institute of Neurological Disorders and Stroke Grants NS-12151, NS-27528, and NS-30549 and a Klingenstein Fellowship in the Neurosciences (I.M.), a Howard Hughes Predoctoral Fellowship (T.S.O.), and a Canadian MRC Postdoctoral Fellowship (Y.D.K.).

1. Bliss, T. V. & Collingridge, G. L. (1993) *Nature (London)* **361**, 31–39.
2. Mody, I. & Heinemann, U. (1987) *Nature (London)* **326**, 701–704.
3. Köhr, G., De Koninck, Y. & Mody, I. (1993) *J. Neurosci.* **13**, 3612–3627.
4. Llano, I., Leresche, N. & Marty, A. (1991) *Neuron* **6**, 565–574.
5. Kano, M., Rexhausen, U., Dreessen, J. & Konnerth, A. (1992) *Nature (London)* **356**, 601–604.
6. Korn, H., Oda, Y. & Faber, D. S. (1992) *Proc. Natl. Acad. Sci. USA* **89**, 440–443.
7. Pitler, T. A. & Alger, B. E. (1992) *J. Neurosci.* **12**, 4122–4132.
8. Stelzer, A., Slater, N. T. & Ten Bruggencate, G. (1987) *Nature (London)* **326**, 698–701.
9. Miles, R. & Wong, R. K. (1987) *Nature (London)* **329**, 724–726.
10. Davies, C. H., Starkey, S. J., Pozza, M. F. & Collingridge, G. L. (1991) *Nature (London)* **349**, 609–611.
11. Mott, D. D. & Lewis, D. V. (1991) *Science* **252**, 1718–1720.
12. Prince, D. A. & Connors, B. W. (1984) *Ann. Neurol.*, Suppl. 16, S59–S64.
13. Lopes da Silva, F. H., Kamphuis, W. & Wadman, W. J. (1992) *Acta Neurol. Scand. Suppl.* **140**, 34–40.
14. Tuff, L. P., Racine, R. J. & Adamec, R. (1983) *Brain Res.* **277**, 79–90.
15. de Jonge, M. & Racine, R. J. (1987) *Brain Res.* **412**, 318–328.
16. Oliver, M. W. & Miller, J. J. (1985) *Exp. Brain Res.* **57**, 443–447.
17. Valdes, F., Dasheiff, R. M., Birmingham, F., Crutcher, K. A. & McNamara, J. O. (1982) *Proc. Natl. Acad. Sci. USA* **79**, 193–197.
18. McNamara, J. O., Peper, A. M. & Patrone, V. (1980) *Proc. Natl. Acad. Sci. USA* **77**, 3029–3032.
19. Shin, C., Pedersen, H. B. & McNamara, J. O. (1985) *J. Neurosci.* **5**, 2696–2701.
20. Tuff, L. P., Racine, R. J. & Mishra, R. K. (1983) *Brain Res.* **277**, 91–98.
21. Busch, C. & Sakmann, B. (1990) *Cold Spring Harbor Symp. Quant. Biol.* **55**, 69–80.
22. Edwards, F. (1991) *Nature (London)* **350**, 271–272.
23. Land, B. R., Salpeter, E. E. & Salpeter, M. M. (1980) *Proc. Natl. Acad. Sci. USA* **77**, 3736–3740.
24. Sigworth, F. J. (1980) *J. Physiol. (London)* **307**, 97–129.
25. Robinson, H. P., Sahara, Y. & Kawai, N. (1991) *Biophys. J.* **59**, 295–304.
26. Traynelis, S. F., Silver, R. A. & Cull-Candy, S. G. (1993) *Neuron* **11**, 279–289.
27. De Koninck, Y. & Mody, I. (1994) *J. Neurophysiol.* **71**, 1318–1335.
28. Racine, R. J. (1972) *Electroencephalogr. Clin. Neurophysiol.* **32**, 281–294.
29. Kairiss, E. W., Racine, R. J. & Smith, G. K. (1984) *Brain Res.* **322**, 101–110.
30. Otis, T. S. & Mody, I. (1992) *Neuroscience* **49**, 13–32.
31. Staley, K. J., Otis, T. S. & Mody, I. (1992) *J. Neurophysiol.* **67**, 1346–1358.
32. Köhr, G. & Mody, I. (1991) *J. Gen. Physiol.* **98**, 941–967.
33. Faber, D. S., Young, W. S., Legendre, P. & Korn, H. (1992) *Science* **258**, 1494–1498.
34. Colquhoun, D. & Hawkes, A. G. (1982) *Philos. Trans. R. Soc. London B* **300**, 1–59.
35. Press, W. H., Teukolsky, S. A., Vetterling, W. T. & Flannery, B. P. (1992) *Numerical Recipes in C: The Art of Scientific Computing* (Cambridge Univ. Press, Cambridge, U.K.), 2nd Ed.
36. Colquhoun, D. & Sigworth, F. J. (1983) in *Single Channel Recording*, eds. Sakmann, B. & Neher, E. (Plenum, New York), pp. 191–263.
37. Edwards, F. A., Konnerth, A., Sakmann, B. & Busch, C. (1990) *J. Physiol. (London)* **430**, 213–249.
38. Gray, R. & Johnston, D. (1985) *J. Neurophysiol.* **54**, 134–142.
39. Maconochie, D. J., Zempel, J. M. & Steinbach, J. H. (1994) *Neuron* **12**, 61–71.
40. Edwards, F. A. & Stern, P. (1991) in *Excitatory Amino Acids and Synaptic Transmission*, eds. Wheal, H. V. & Thomson, A. M. (Academic, New York), pp. 171–196.
41. Verdoorn, T. A., Draguhn, A., Ymer, S., Seeburg, P. H. & Sakmann, B. (1990) *Neuron* **4**, 919–928.
42. Korn, H., Bausela, F., Charpier, S. & Faber, D. S. (1993) *J. Neurophysiol.* **70**, 1249–1254.
43. Wyllie, D. J. A., Manabe, T. & Nicoll, R. A. (1994) *Neuron* **12**, 127–138.
44. Toyoshima, C. & Unwin, N. (1988) *Nature (London)* **336**, 247–250.
45. Unwin, N. (1993) *J. Mol. Biol.* **229**, 1101–1124.
46. Kosaka, T., Hama, K. & Wu, J. Y. (1984) *Brain Res.* **293**, 353–359.
47. Green, W. N., Ross, A. F. & Claudio, T. (1991) *Neuron* **7**, 659–666.
48. Kirsch, J., Wolters, I., Triler, A. & Betz, H. (1993) *Nature (London)* **366**, 745–748.
49. Manabe, T., Renner, P. & Nicoll, R. A. (1992) *Nature (London)* **355**, 50–55.